Available online at www.sciencedirect.com
SCIENCE DIRECT®
Chemical Physics Letters 368 (2003) 331–337
CHEMICAL PHYSICS LETTERS
www.elsevier.com/locate/cplett

Fabrication of inorganic molybdenum disulfide fullerenes by arc in water

Noriaki Sano [a,b,1], Haolan Wang [a], Manish Chhowalla [a,*], Ioannis Alexandrou [a], Gehan A.J. Amaratunga [a], Masakazu Naito [b], Tatsuo Kanki [b]

[a] *Engineering Department, University of Cambridge, Trumpington Street, Cambridge CB2 1PZ, UK*
[b] *Chemical Engineering Department, Himeji Institute of Technology, 2167 Shosha, Himeji, 671-2201 Japan*

Received 9 October 2002; in final form 21 November 2002

Abstract

Closed caged fullerene-like molybdenum disulfide (MoS_2) nano-particles were obtained via an arc discharge between a graphite cathode and a molybdenum anode filled with microscopic MoS_2 powder submerged in de-ionized water. A statistical study of over 150 polyhedral fullerene-like MoS_2 nano-particles in plan view transmission electron microscopy revealed that the majority consisted of 2–3 layers with diameters of 5–15 nm. We show that the nano-particles are formed by seamless folding of MoS_2 sheets. A model based on the agglomeration of MoS_2 fragments over an extreme temperature gradient around a plasma ball in water is proposed to explain the formation of nano-particles.

1. Introduction

The extraordinary properties of carbon fullerenes and nanotubes make them ideal for wide ranging applications [1–3]. This has prompted efforts to develop simple and cheap methods for large-scale production of these materials [4–6]. It is now recognized that polyhedral closed caged nano-structures under certain energetic considerations are thermodynamically more stable than isolated basal sheets of the lamellar structure. The propensity of graphite to form hollow closed structures is believed to stem from the high energy of the dangling bonds at the edge of the graphene planes [7]. Since this is also true for other inorganic layered structures, the formation of closed caged nano-particles is a general property of all materials with anisotropic two-dimensional layered structures. This has led to the generation of numerous types of closed nano-structures from materials such as MoS_2 [8], BN [9], $NiCl_2$ [10] and GaSe [11]. These materials have novel properties that make them ideal for many optical, electronic and mechanical applications. However, in order to utilize these materials for practical applications, large quantities are desired.

Tenne and co-workers [8,12–14] have developed a method for large-scale fabrication of inorganic fullerenes (IF) such as MoS_2 and WS_2. They have

* Corresponding author. Fax: +441223332662.
E-mail addresses: sano@mech.eng.himeji-tech.ac.jp (N. Sano), mc209@cam.ac.uk (M. Chhowalla).
[1] Also corresponding author.

0009-2614/02/$ - see front matter
PII: S0009-2614(02)01884-5

shown that spherical nano-particles of WS_2 produced by their process have superior tribological properties [15]. The process consists of sulfidation of WO_{3-x} and MoO_{3-x} precursors through a slow diffusion-controlled reaction. Using this method they are able to generate large quantities of spherical IF with diameters ranging from tens to hundreds of nanometers. They propose that the curvature of the planes forming the shells of the IF nano-particles is induced by reduction of energy through termination of dangling bonds. Conventional methods such as arc discharge in inert gas atmosphere [16] and laser ablation [17] have also been used for the generation of IF MoS_2 nano-particles. In the case of laser ablation, it is conjectured that the smallest single walled IF particle has a size of 4–5 nm [17]. Parilla et al. [17] argue that such a particle may represent the C_{60} of inorganic materials. In contrast to the process of Tenne et al., the conventional methods are non-equilibrium processes and not necessarily governed by thermodynamics alone.

In this Letter, we report an alternative cost-effective method for fabrication of IF nano-particles. The method consists of a simple apparatus that does not require harmful gases, vacuum equipment or costly lasers. Our method of submerged arc discharge has the ability to produce large quantities of IF nano-particles in a cost-effective manner. This could lead to their use in wide ranging applications.

In our previous report [18,19], we showed that an arc discharge between two carbon electrodes submerged in water yields large quantities of carbon bucky 'onions'. Here we report on similar experiments to produce MoS_2 nano-particles using this simple and cost-effective technique. Our results show that it is possible to fabricate closed caged MoS_2 nano-particles with a relatively uniform size distribution from 2H MoS_2 powder. Based on these results we believe that it will be possible to fabricate large quantities of nano-particles using this technique.

2. Experimental details

We have used the same apparatus to fabricate MoS_2 nano-particles as that used for producing carbon bucky 'onions' [18,19]. Briefly, a 3 l Pyrex beaker was filled with 2500 cm^3 of de-ionized water. A high-purity (99.99%) graphite rod (diameter of 12 mm and length of 20 mm) was used as the cathode and a high-purity (99.9%) Mo rod (7 mm in diameter and 80 mm in length) was used as the anode. A hole with a diameter of 5 mm and a depth of 50 mm was drilled into the Mo rod. The hollow Mo anode was then filled with a 44 μm 2H MoS_2 powder that was compacted using nominal force. Both electrodes were submerged in water and the arc was initiated by touching the Mo anode to the stationary graphite cathode. The arc current of 30 A and an arc voltage of 17 V were supplied by a direct current (d.c.) welding power supply.

A blue plasma emission was readily observed during the arc discharge. The discharge here, in contrast to the carbon arc, was very unstable and frequent re-triggering was required in order to maintain the plasma. The instability in the arc was attributed to the rapid change in the distance between the cathode and the anode due to the erosion of the Mo anode. The melting of the Mo anode indicates that the local temperature of the discharge is greater than 2900 K, the melting temperature of Mo. Immediately following the discharge, a transparent powder floating on the water surface could be seen. No other powder or discoloration of the cathode or the anode was visible, indicating that most of the vaporized products were released into the water during the discharge. Similar to the carbon 'onions' the MoS_2 nano-particles also tend to migrate to the water surface. Negligible amount of powder was found at the bottom of the beaker or as suspension in the water. Finally, a quadrapole mass spectrometer (M-QA200TS, ANELVA) was used to detect the emitted vapor during the discharge in order to gain insights into the reactions occurring in the plasma zone.

3. Results and discussion

The powder from the water surface was transferred directly onto a holey carbon grid without any purification. The microscopy was performed on JEOL4000EX and JEOL2010 transmission electron microscope (TEM) operated at 400 and 200 keV, respectively. The TEM image of the

floating product collected from the surface of the water is shown in Fig. 1. Fullerene-like particles with apparently different sizes and shapes can be readily observed along with lamellar MoS_2 crystals. The IF nano-particles were confirmed to be MoS_2 by measuring the spacing between the planes. The average distance between the curved planes was found to be 6.25 Å, close to that of 2H MoS_2 crystal (6.15 Å). The slight expansion of the lattice spacing in the closed MoS_2 nano-particles is consistent with the results of Tenne and co-workers [12–14] who observed a shift in the (0 0 0 2) X-ray diffraction peak due to strain relief in curved MoS_2 structures. Furthermore, it was observed that the d-spacing between the layers in regions where the planes curve sharply was significantly larger (up to 10% at 6.83 Å) than in 2H MoS_2 crystals. This expansion may be related to the repulsive forces from close proximity of the atoms in these regions. A statistical study of several images similar to that shown in Fig. 1 was carried out in order to obtain information that may be helpful in elucidating a growth mechanism. The results of the statistical study of over 150 nano-particles are summarized in Fig. 2. It shows that the projected 2D shape of the 3D nano-particles is predominantly tetragonal (~70% from Fig. 2a). Furthermore, the results indicate that the majority of the particles (~75%) have only 2–3 layers and range in size from 5 to 15 nm. The fact that the distribution of shapes and sizes is fairly narrow indicates a consistent formation process. It may also point to stable nano-structures of MoS_2 that are preferred over less energetically favorable ones. However, care must be taken when interpreting the HREM

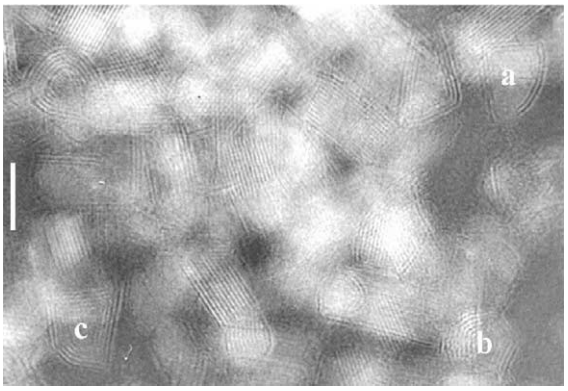

Fig. 1. Transmission electron microscopy image of MoS_2 nano-particles generated using the arc in water. The particles labelled as a, b and c represent triangular, hexagonal and pentagonal projected shapes. The scale bar corresponds to 10 nm.

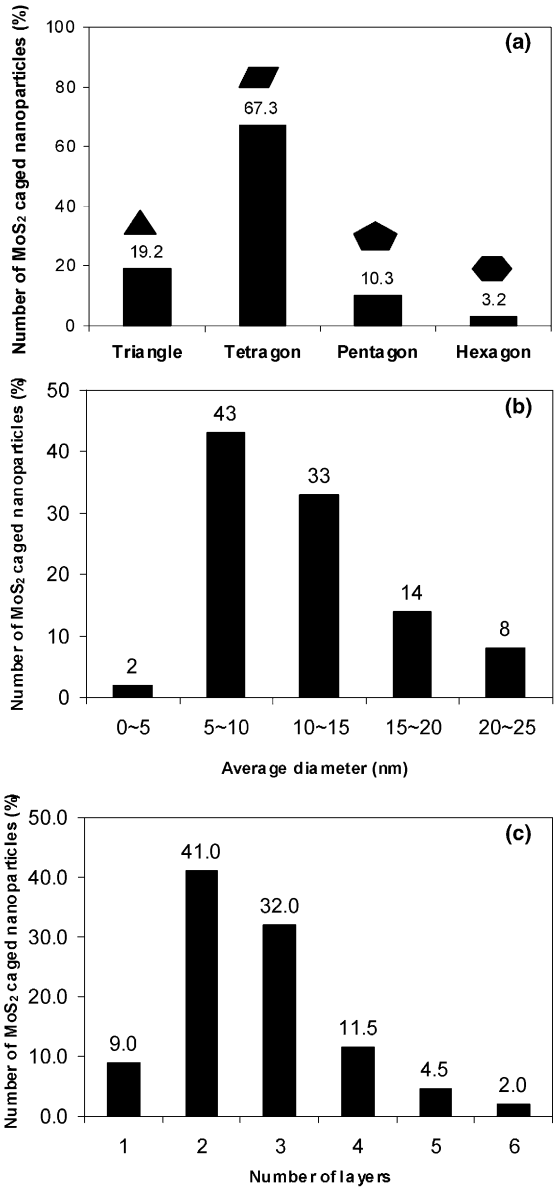

Fig. 2. Statistical distributions of nano-particle (a) shapes, (b) size and (c) number of layers.

images because TEM images are 2D projections of 3D objects and so the shape of the object being viewed depends on the orientation of that object with respect to the electron beam. Therefore the same object can have different shapes if oriented differently. Fig. 3 shows an example of how tilting of the specimen with respect to the electron beam in a TEM apparently changes the shape of the nano-particle. Here, the shape of the particle changes from a pentagonal polyhedron to one with six sides with tilting.

A 2D MoS_2 plane has some structural features, one of which is that three-membered Mo rings which have two S atoms in its cell must not be adjacent one another. Several caged MoS_2 structures can be possible under this limitation using a single MoS_2 sheet connected seamlessly so that the surface energy of the particle is minimized. A typical structure in accordance with this limitation is the regular octahedral cage proposed by Parilla et al. [17]. However, it is in our HREM observations many of the particles have elongated shapes that do not match the projection of the octahedral structure. We show that the polyhedral structures observed here can be reconstructed using a single seamless MoS_2 sheets. The upper panel of Fig. 4 shows photographs of models we have constructed to elucidate the wrapping MoS_2 sheets which could give rise to the IF nano-particle shapes observed in the TEM and shown in the lower panel of Fig. 4. The lines on the constructed structures (upper panel of Fig. 4) represent Mo planes, and the circles indicate sulfur atoms. The models in the upper panel of Fig. 4 show MoS_2 sheets that are connected seamlessly except at vertices where three or four sheets are joined. These vertices consist of four or five-member Mo rings because de-atomization at the vertices is required to avoid excessively close proximity of atoms. The model structures shown in the upper panel closely match the observed TEM images and therefore can be used to explain the structure of the generated IF nano-particles. In addition to the structures and shapes shown in Fig. 4, we have also confirmed the structure of other IF nano-particle shapes using the seamless models. This result indicates that the surface energy of many of the MoS_2 nano-particles produced in the submerged arc method is minimized via termination of dangling bonds during their formation. A thorough structural study with energetic and electronic calculations is currently in progress, and these results will be reported elsewhere. In addition, a detailed crystallographic study based on examination of high-resolution TEM images is underway.

4. Formation mechanism

Based on our observations, we propose a growth mechanism for the formation of hollow MoS_2 nano-particles in the submerged arc system. The model shown schematically in Fig. 5 consists of three stages, which continuously occur in the

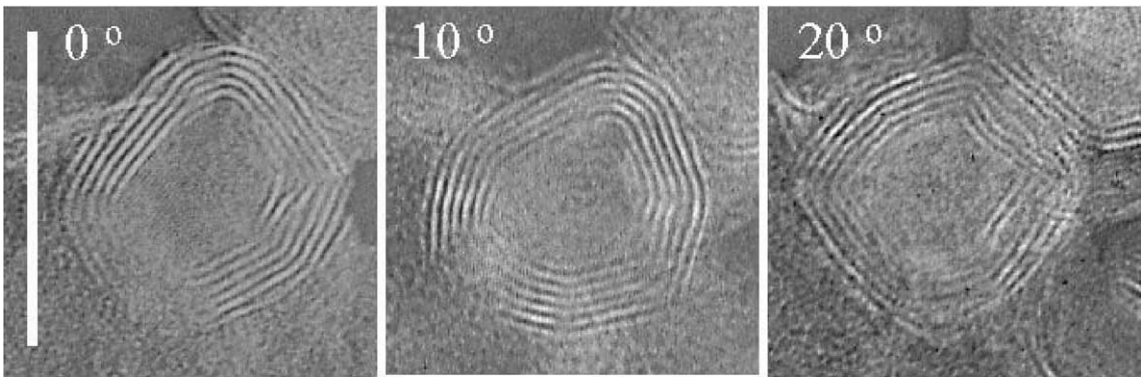

Fig. 3. TEM images of a MoS_2 nano-particle tilted at three different angles. The scale bar corresponds to 20 nm.

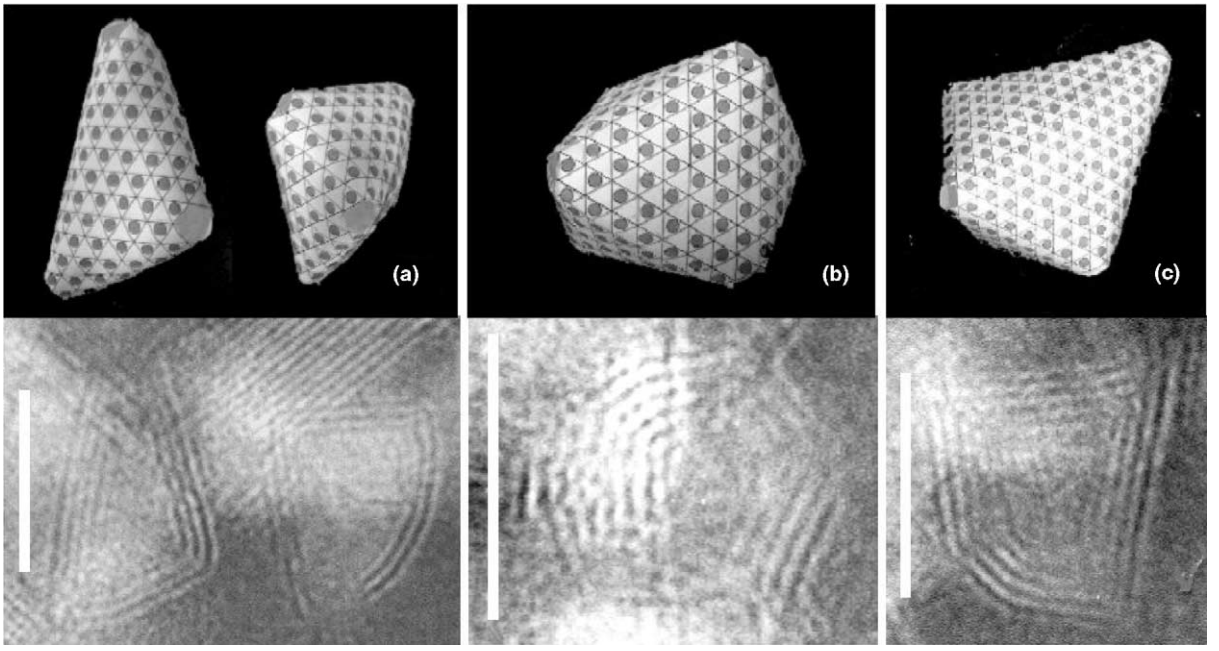

Fig. 4. The upper panel shows constructed models used to explain the different MoS_2 nano-particle shapes observed in the TEM. The lines in the upper panel models represent the Mo planes while the closed circles represent the sulfur atoms. The models were constructed by seamless closing of MoS_2 sheets. The lower panel shows the actual TEM image of the observed MoS_2 nano-particles of different shapes. The scale bar in each figure corresponds to 10 nm.

gas phase within the reaction bubble surrounding the discharge. The first stage in the formation of MoS_2 nano-particles is the generation of the MoS_2 vapor in the hot plasma zone. As the arc is initiated bubbles are released indicating the presence of vapor. The composition of this vapor is presently not known but based on the materials present it may be inferred that it consists of H_2O, H_2, H_2S, MoS_2, Mo and S and other combinations of these materials as well as their ionic states. The residual gas components in the bubbles exhibited mass numbers of 48, 60, 64 and 76, correlating to several sulfuric compounds such as CH_3SH, COS, S_2, and CS_2. However, excessive background noise in the mass spectra made it difficult to extract peaks from expected gases, such as H_2S, H_2, H_2, O_2, H_2O. Currently, detailed gas analysis is under way using chromatography. As the temperature exceeds 3000 K, a bubble of vapor displaces the liquid near the discharge. The pressure within this gas bubble is expected to be close to one atmosphere. It must be noted that the discharge in our case is an anodic arc where the anode is vaporized through thermal evaporation rather than the violent ablation found in the cathodic arc discharge. In this case, we expect molecules of MoS_2 along with atoms of the constituent species since the temperature of the discharge exceeds the boiling point of 2H MoS_2 crystal (2650 K). However, in contrast to low-pressure cathodic arc plasmas, we do not expect to have significant number of very high-energy ions in our discharge. In such conditions it is reasonable to assume that nanometer sized fragments of MoS_2 may also be generated. In stage 2 of our phenomenological model, the evaporated material expands rapidly away from the plasma zone in a manner that is typical for arc plasmas [20]. As the vapor expands, it is quenched. The quenching zone surrounding the plasma zone is labelled in Fig. 5. In the quenching zone, the constituent species begin to agglomerate driven by the requirement for a lower energy state through passivation of dangling bonds. This leads to the formation of larger fragments.

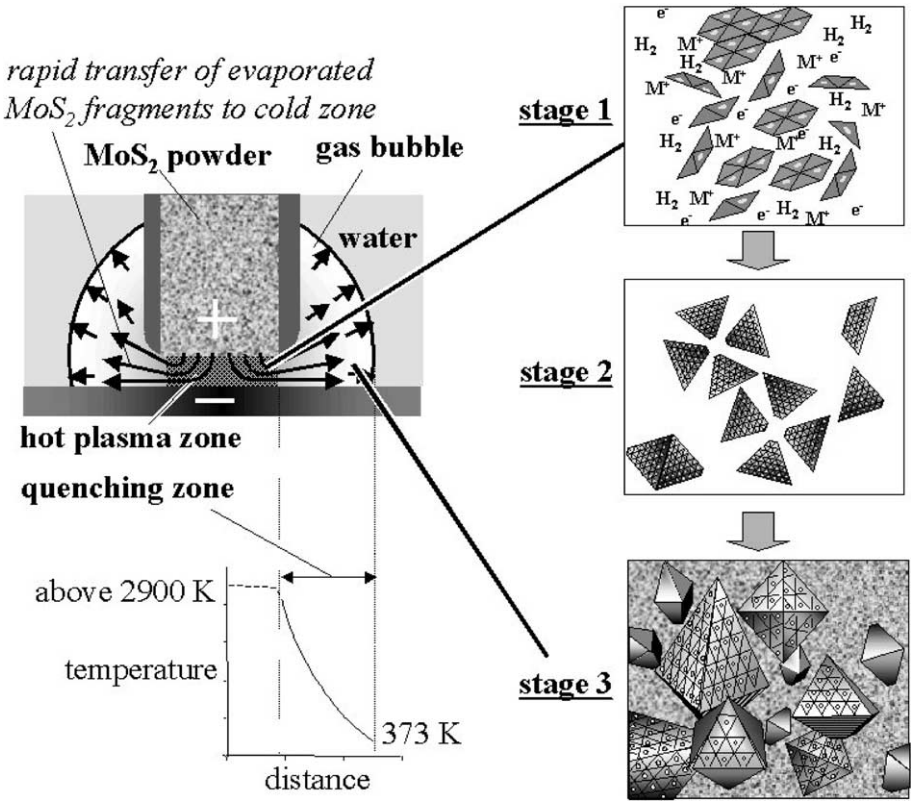

Fig. 5. Schematic of the empirical model showing the formation mechanism of MoS_2 nano-particles.

In stage 3, as these fragments reach a critical size, closed caged particles can be formed to eliminate the remaining dangling bonds and further reduce the energy of the system (stage 3 in Fig. 5). A critical minimum size of the nano-particles is required for the formation of closed caged structures in MoS_2 due to structural angle and bond length limitations. The curvature of very small fragments (less than 5 nm) increases the proximity of neighboring atoms inducing large strain in the structures making them highly unstable.

The fact that we see from Fig. 2b that most of the closed nano-particles are in the size range of 5–15 nm appears to indicate that in our case, the critical size for the formation of closed nano-particles is 5 nm. This is also in agreement with the results of Parilla et al. [17] who argue that a MoS_2 nano-particle with a size of 4–5 nm may be the smallest stable inorganic fullerene. This is also supported by the fact that a significant lattice expansion (up to 10%) is observed at the vertices of nano-particles. The fact that we do not see many larger closed nano-particles appears to indicate that as the agglomerates grow above some critical size, the surface energy due to dangling bonds is offset by the internal energy gain by the crystal. However, the size distribution of the closed nano-particles will also depend on the agglomeration of MoS_2 fragments, which in turn is determined by the quench rate. That is, if the plasma and quenching zones in Fig. 5 were somehow expanded, it may lead to larger nano-particles. Therefore, unlike the process of Tenne and co-workers [12–14] where the size of the IF nano-particles is determined by the initial oxide particles, here the size distribution is determined by the non-equilibrium plasma conditions.

5. Conclusions

In conclusion, we show that a relatively simple and cheap technique of an arc discharge submerged in water is effective for generating MoS_2 inorganic fullerenes. The method yields MoS_2 nano-particles with mostly 2–3 layers and size of 5–15 nm. It was shown that structural models constructed using closed seamless MoS_2 sheets match the shapes of MoS_2 fullerenes observed in TEM. Based on these observations, a growth model based on agglomeration of MoS_2 fragments and formation of closed nano-particles at some critical size based on the quench rate is proposed. It is argued that the process is driven by energy minimization through passivation of dangling bonds.

References

[1] F. Diederich, C. Thilgen, Science 271 (1996) 317.
[2] P.G. Collins, K. Bradley, M. Ishigami, A. Zettl, Science 287 (2000) 1801.
[3] P.L. McEuen, Nature 393 (1998) 15.
[4] W. Kratschmer, L.D. Lamb, K. Fostiropoulos, D.R. Huffman, Nature 347 (1990) 354.
[5] R.E. Haufler, J. Conceicao, L.P.F. Chibante, Y. Chai, N.E. Byrne, S. Flanagan, M.M. Haley, S.C. O'Brien, C. Pan, Z. Xiao, W.E. Billups, M.A. Cufolini, R.H. Hauge, J.L. Margrave, L.J. Wilson, R.F. Curl, R.E. Smalley, J. Phys. Chem. 94 (1990) 8634.
[6] H.J. Dai, A.G. Rinzler, P. Nikolaev, A. Thess, D.T. Colbert, R.E. Smalley, Chem. Phys. Lett. 260 (1996) 471.
[7] D.H. Robertson, D.W. Brenner, C.T. White, J. Phys. Chem. 96 (1992) 6133.
[8] R. Tenne, L. Margulis, M. Genut, G. Hodes, Nature 360 (1992) 444.
[9] N.G. Chopra, R.J. Luyken, K. Cherrey, V.H. Crespi, M.L. Cohen, S.G. Louie, A. Zettl, Science 269 (1995) 966.
[10] Y.R. Hacohen, E. Grunbaum, R. Tenne, J. Sloan, J.L. Hutchison, Nature 395 (1998) 336.
[11] M. Cote, M.L. Cohen, D.J. Chadi, Phys. Rev. B 58 (1998) R4277.
[12] Y. Feldman, E. Wasserman, D.J. Srolovitz, R. Tenne, Science 267 (1995) 222.
[13] Y. Feldman, G.L. Frey, M. Homyonfer, V. Lyakhovitskaya, L. Margulis, H. Cohen, G. Hodes, J.L. Hutchison, R. Tenne, J. Am. Chem. Soc. 118 (1996) 5362.
[14] A. Zak, Y. Feldman, V. Alperovich, R. Rosentsveig, R. Tenne, J. Am. Chem. Soc. 122 (2000) 11108.
[15] L. Rapoport, Y. Bilik, Y. Feldman, M. Homyonfer, S.R. Cohen, R. Tenne, Nature 387 (1997) 791.
[16] M. Chhowalla, G.A.J. Amaratunga, Nature 407 (2000) 164.
[17] P.A. Parilla, A.C. Dillon, K.M. Jones, G. Riker, D.L. Schulz, D.S. Ginley, M.J. Heben, Nature 397 (1999) 114.
[18] N. Sano, H. Wang, M. Chhowalla, I. Alexandrou, G.A.J. Amaratunga, Nature 414 (2001) 506.
[19] N. Sano, H. Wang, M. Chhowalla, I. Alexandrou, G.A.J. Amaratunga, J. Appl. Phys. 92 (2002) 2783.
[20] M. Chhowalla, C.A. Davis, M. Weiler, B.Y. Kleinsorge, G.A.J. Amaratunga, J. Appl. Phys. 79 (1996) 2237.